Journal of Crystal Growth 124 (1992) 176–180
North-Holland

JOURNAL OF CRYSTAL GROWTH

Chemical beam epitaxy of GaInP on GaAs(100) substrates and its application to 0.98 μm lasers

R.M. Kapre, W.T. Tsang, Y.K. Chen, M.C. Wu, M.A. Chin [1] and F.S. Choa [2]
AT&T Bell Laboratories, Murray Hill, New Jersey 07974, USA

We present results on the growth, doping, and application to lasers of GaInP on GaAs(100) substrates using chemical beam epitaxy (CBE). The growth studies were performed in the substrate temperature range of 490–555°C. We were able to obtain lattice-matching with good surface morphology over the entire substrate range investigated. For a fixed triethylgallium (TEGa) flow, a sharp increase in the trimethylindium (TMIn) flow required to obtain lattice-matching for T_{sub} above 520°C is observed. This can be attributed to an increase in GaP growth rate and a decrease in InP growth rate due to desorption of TMIn species. The p-type and n-type doping of $Ga_{0.51}In_{0.49}P$ was investigated using diethylzinc (DEZn) and hydrogen sulfide (H_2S), respectively. It was found that low substrate temperature ($\lesssim 510$°C) was necessary to obtain high p-type doping. Separate confinement heterostructure (SCH) lasers with strained $In_{0.2}Ga_{0.8}As/GaAs$ multiple-quantum-well (MQW) active layers and $Ga_{0.51}In_{0.49}P$ cladding layers for operation at 0.98 μm were grown. Broad-area lasers show extremely low threshold current densities, J_{th}, of 70 A/cm^2. Ridge waveguide lasers with 4 μm stripe width have a threshold of 7.8 mA and gave linear CW output powers upto 100 mW. High external quantum efficiency of 0.9 mW/mA and a very low internal waveguide loss of 2.5 cm^{-1} were obtained from these lasers.

1. Introduction

The vast majority of compound semiconductor devices grown on GaAs substrates make use of AlGaAs as the wide-band-gap semiconductor. A promising alternative to AlGaAs as a wide-band-gap material is GaInP lattice matched to GaAs substrates. The significant advantages of GaInP include low deep level concentrations [1], a large valence band discontinuity, and a lower reactivity with carbon and oxygen than AlGaAs. Very low recombination velocities (< 1.5 cm/s) have been reported at the GaInP/GaAs interface [2]. These advantages make GaInP a very attractive material for lasers. The large ΔE_v makes it suitable for heterojunction bipolar transistor applications without the need for compositionally graded wide bandgap emitters, and the large ΔE_c (0.2 eV) and ΔE_v (0.285 eV) [3] make it suitable for complementary device applications. The vast majority of the work on this material system has been done using metalorganic vapor phase epitaxy (MOVPE), however some work has also been done using chemical beam epitaxy (CBE) [4,5]. We have investigated the growth and doping of GaInP on GaAs substrates using CBE.

Strained InGaAs/AlGaAs quantum well (QW) lasers are currently of great interest because the emission wavelength can be extended to ~ 1.1 μm, beyond the long-wavelength limit of ~ 0.89 for GaAs/AlGaAs lasers. Such extension of wavelength by the addition of In to the GaAs active layer of GaAs/AlGaAs lasers was first proposed and demonstrated in 1981 by Tsang [6]. Recently there has been a lot of interest in using these strained QW lasers operating at 0.98 μm due to their suitability for pumping erbium-doped fiber amplifiers [7,8]. They yield a lower noise figure and higher gain coefficient than the 1.48 μm InGaAs/InP pump lasers [7] as well as 0.8 μm AlGaAs/GaAs pump lasers [8]. In addition,

[1] Present address: University of California, Santa Barbara, California, USA.
[2] Present address: University of Maryland, Baltimore, Maryland, USA.

the InGaAs/AlGaAs strained QW lasers have lower threshold current, higher slope efficiency, and less temperature dependance. All these factors contribute to lowering the power dissipation of the pump design. Recently $Ga_{0.51}In_{0.49}P$, lattice-matched to GaAs has been introduced as a substitute for the AlGaAs cladding layers due to reports suggesting their resistance to rapid degradation by dark line defect propagation [9] and to catastrophic mirror damage [10]. The aluminium-free system also lends itself more readily to device fabrication by selective etching and epitaxial regrowth or mass transport [11]. Lasers with GaInP cladding layers have been grown by MOVPE [9,11] and gas-source molecular beam epitaxy (GSMBE) [12]. We report on the first InGaAs/GaAs strained-layer QW lasers using $Ga_{0.51}In_{0.49}P$ cladding layers grown by CBE [13,14].

2. Experimental procedure

The material was grown using a modified Riber 32 CBE system. The group III sources were trimethylindium (TMIn) and triethylgallium (TEGa), the group V sources were arsine (AsH_3), phosphine (PsH_3), while the dopant sources were diethylzinc (DEZn) and hydrogen sulfide (H_2S). Lattice matching of GaInP was investigated using X-ray crystallography. The substrate temperature, T_{sub}, was measured and controlled using an infra-red pyrometer.

2.1. Growth of GaInP on GaAs(100)

The GaInP layers were grown to a thickness of about 1 μm at a growth rates varying from ~ 6 to 10 Å/s. The substrate temperature range investigated was 490–555°C. The H_2 + TEGa (~ 10% concentration) flow rate was kept fixed at 12 SCCM, while the H_2 + TMIn (~ 5.5% concentration) flow rate was adjusted to obtain lattice matching at various substrate temperatures. A plot of H_2 + TMIn flow rate required to achieve lattice matching within 0.15% versus T_{sub} for a fixed PH_3 flow of 10 SCCM is shown in fig. 1. The full width at half maximum (FWHM) of the X-ray diffracted intensity from the epilayers was

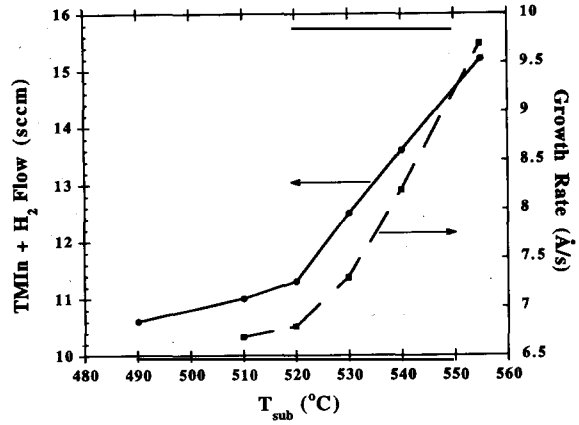

Fig. 1. The substrate temperature dependance of the H_2 + TMIn flow required to obtain lattice matching of GaInP on n^+-GaAs substrate and the $Ga_{0.51}In_{0.49}P$ growth rate. The H_2 + TEGa flow and PH_3 flow were kept constant at 12 and 10 SCCM, respectively.

about 20″. We find that at temperatures higher than 520°C there is a sharp increase in the flow rate required to obtain lattice matching. This observation is similar to that reported by Garcia et al. [5]. The growth rate of the $Ga_{0.51}In_{0.49}P$ epilayers at the various T_{sub} is also plotted in fig. 1. It can be seen that the growth rate increases with increasing T_{sub} much the same way as the TMIn + H_2 flow required to obtain lattice-matching to GaAs. This suggests that the increased TMIn flow is required primarily to compensate for the increased Ga incorporation with increasing T_{sub}. Some of the increased TMIn flow is also necessary to compensate for increased desorption of In species at higher T_{sub}. The growth rate increase of GaP and growth rate decrease of InP with increasing substrate temperature in the range of 500–550°C has been reported by Garcia et al. [15]. Increasing the PH_3 flow from 10 SCCM to 20 SCCM at a T_{sub} of 555°C resulted in a decrease in indium composition from 49% to 44%. We were able to obtain material with mirror smooth morphology without a significant density of defects over the entire temperature range investigated (490–555°C).

2.2. Doping of $Ga_{0.51}In_{0.49}P$

The p-doping of GaInP was achieved using DEZn + H_2 (~ 27% concentration) and the

doped films grown on semi-insulating substrates were characterized using Hall measurements. A plot of the hole concentration dependance on T_{sub} for a fixed DEZn flow of 3 SCCM is shown in fig. 2. The growth rate of GaInP for this study was ~ 6.5 Å/s. The p-doped films had mobilities varying from 40 to 20 $cm^2/V \cdot s$ for doping densities varying from 2×10^{16} to 5×10^{18} cm^{-3}. The n-type doping in the 10^{18} cm^{-3} range of GaInP could be obtained easily for T_{sub} up to 550°C using $H_2S + H_2$ (~ 0.3% concentration) flows of less than 5 SCCM.

2.3. Laser structure growth and device performance

The laser structure is a separate confinement heterostructure (SCH) to provide confinement of electrical carriers as well as the optical field. The cross-section of the InGaAs/GaAs/GaInP laser after fabricating into a ridge waveguide structure is shown in fig. 3. First a 0.2 μm thick n^+-GaAs buffer layer was grown on n^+-GaAs substrate, followed by a 1.35 μm thick n-$Ga_{0.51}In_{0.49}P$ cladding layer and a 0.1 μm thick n-GaAs waveguide layer. This was followed by the active region consisting of one, two or three 70 Å thick $In_{0.2}Ga_{0.8}As$ quantum wells and 220 Å thick GaAs barriers. A 0.1 μm thick p-GaAs waveguide, 1.35 μm thick p-$Ga_{0.51}In_{0.49}$ cladding layer and 0.2 μm thick p^+-GaAs contact layer completed the structure. The doping in the waveguide layers was set-back from the active region by about 50 Å to prevent dopant diffusion into it. The growth was done at T_{sub} of 540°C except for the p-GaInP which was grown at 510°C to permit sufficient Zn incorporation. The growth rates used were 5.5 Å/s for GaAs, 4.5 Å/s for InGaAs, 8.2 Å/s for n-GaInP, and 6.7 Å/s for p-GaInP. To facilitate ridge waveguide laser fabrication, a thin GaAs stop-etch layer was inserted in the upper GaInP cladding layer. Ridge waveguides of 4 μm width were formed by selective wet chemical etching, then the wafer was covered by Si_3N_4 and a self-aligned process was used to define p-contact opening on top of the ridge. Standard metallization and cleaving processes were used to finish the laser fabrication.

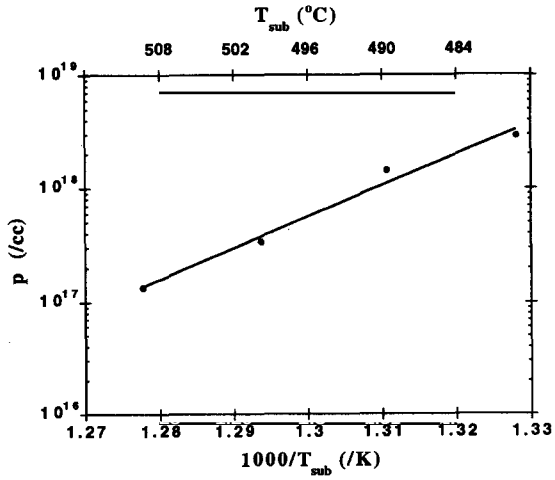

Fig. 2. The net hole concentration dependance on the substrate temperature for a fixed diethylzinc flow of 3 SCCM and GaInP growth rate of ~ 6.5 Å/s.

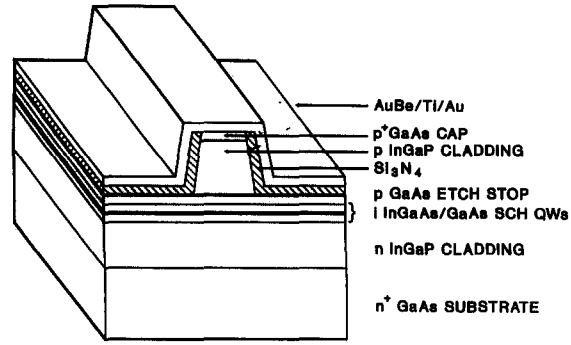

Fig. 3. The schematic of the self-aligned ridge waveguide InGaAs/GaAs quantum well laser with lattice-matched GaInP cladding layers.

The cavity length dependance of the threshold current density, J_{th}, for broad-area lasers having single and two quantum wells is shown in fig. 4. A very low J_{th} of 70 A/cm^2 was obtained for a 1500 μm long single QW laser which is among the lowest reported for InGaAs/GaAs/GaInP lasers. The values of J_{th} for two and three QW lasers were 135 and 170 A/cm^2 respectively. For comparison, values of J_{th} of 70 and 177 A/cm^2 were obtained by MOVPE [9] for single QW laser and by GSMBE [12] for three QW laser, respectively. As compared to devices with AlGaAs cladding

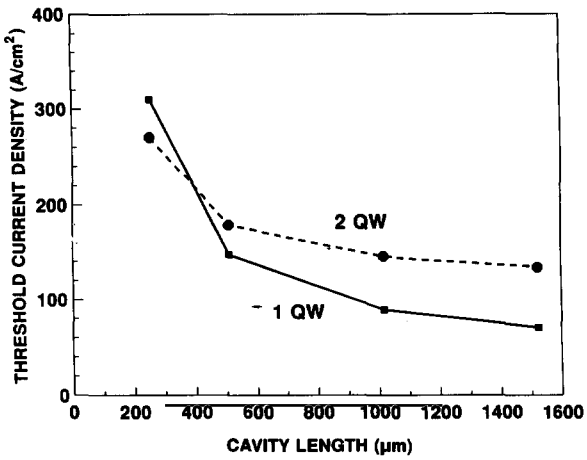

Fig. 4. The cavity length dependence of the threshold current densities, J_{th}, for broad-area lasers having a single and two quantum wells.

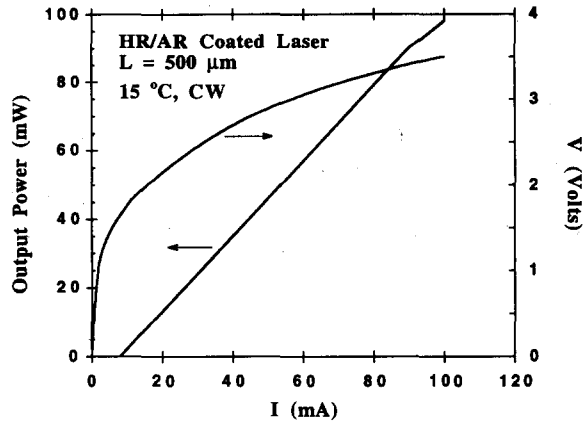

Fig. 5. A typical CW light–current characteristic for a 500 μm long single QW ridge waveguide (4 μm wide) laser with high-reflective(85%)/anti-reflective(5%) coated facets.

layers, the present J_{th} is among the best values of 65 A/cm^2 obtained by MOVPE [16] and ~50 A/cm^2 by MBE [17,18].

The ridge waveguide lasers have very low CW threshold currents: 7.8 mA for 500 μm long cavity and 10 mA for 750 μm long cavity. Such values are lower than those obtained from similar laser structures grown by GSMBE [12]. A typical CW light–current characteristic for 500 μm long lasers with high-reflective(~ 85%)/anti-reflective(~ 5%) coating is shown in fig. 5. They emitted linear CW output powers up to 100 mW. The lasing wavelength obtained was 0.98 μm. Higher output power was possible but higher order transverse mode set in. External differential quantum efficiency as high as 0.9 mW/mA was obtained for 250 μm long lasers. Fig. 6 shows the CW threshold currents and the inverse of external quantum efficiency for single QW ridge waveguide lasers as a function of cavity length. From the slope of inverse quantum efficiency versus cavity length, a very low internal waveguide loss α_i of 2.5 cm^{-1} and internal quantum efficiency η_i of 0.95 were measured. The present value of α_i is the lowest reported. Values of α_i of 5 and 9 cm^{-1} were previously reported for MOVPE grown InGaAs/GaAs/AlGaAs lasers [16] and GSMBE-grown InGaAs/GaAs/GaInP lasers [12], respectively. The temperature dependence of CW threshold currents and external quantum efficiencies of a 750 μm long ridge waveguide laser were studied by varying the heat-sink temperature. The diode was bonded p-side up on copper heat-sink. A threshold-temperature dependence coefficient, T_0 of 90 K was measured. At 100°C the external quantum efficiency stayed at ~ 0.8 mW/mA.

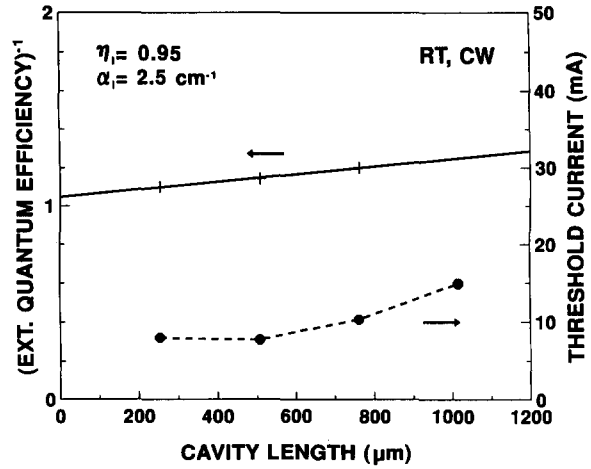

Fig. 6. The inverse external differential quantum efficiency and the threshold current versus the cavity length for single QW ridge waveguide lasers. The extrapolated internal quantum efficiency is 95% and the internal waveguide loss is 2.5 cm^{-1}.

3. Summary and conclusions

In summary, high quality growth of GaInP on GaAs(100) substrates was accomplished. Lattice-matching with good surface morphology was obtained over a substrate temperature range of 490–555°C. Both p-type and n-type doping of GaInP was accomplished using gaseous source dopants. Strained InGaAs/GaAs MQW lasers with $Ga_{0.51}In_{0.49}P$ cladding layers were grown on GaAs substrates using all gaseous source CBE. The single QW broad-area lasers have a very low threshold current density of 70 A/cm^2, among the lowest value reported for InGaAs/GaAs/GaInP lasers. Ridge-waveguide lasers emitting at 0.98 μm have a CW threshold of 7.8 mA for a 500 μm long cavity and a differential quantum efficiency as high as 0.9 mW/mA. Internal quantum efficiency of 0.95 and internal waveguide losses of 2.5 cm^{-1} were obtained. Linear CW output power of 100 mW was obtained. These results demonstrate that CBE is capable of growing 0.98 μm InGaAs strained-layer QW lasers having performance similar to the best prepared by other epitaxial growth techniques.

References

[1] M. Razeghi, P. Maurel, F. Omnes, M. Defour, C. Boothroyd, W.M. Stobbs and M. Kelly, J. Appl. Phys. 63 (1988) 4511.
[2] J.M. Olson, R.K. Ahrenkiel, D.J. Dunlavy, B. Keyes and A.E. Kibbler, Appl. Phys. Letters 55 (1989) 1208.
[3] D. Biswas, N. Debbar, P. Bhattacharya, M. Razeghi, M. Defour and F. Omnes, Appl. Phys. Letters 56 (1990) 833.
[4] K. Ozasa, M. Yuri, S. Tanaka and H. Matsunami, J. Appl. Phys. 65 (1989) 2711.
[5] J.C. Garcia, P. Maurel, P. Bove, J.P. Hirtz and A. Barski, J. Crystal Growth 111 (1991) 578.
[6] W.T. Tsang, Appl. Phys. Letters 38 (1981) 661.
[7] M. Shimizu, M. Horiguchi, M. Yamada, M. Okayasu, T. Takeshita, I. Nishi, S. Uehara, J. Noda and E. Sugita, Electron. Letters 26 (1990) 498.
[8] B. Pederson, B.A. Thompson, S. Zemon, W.J. Miniscalco and T. Wei, IEEE Photon. Technol. Letters PTL-4 (1992) 46.
[9] T. Ijichi, M. Ohkubo, N. Matsuoto and H. Okamoto, in: Proc. 12th IEEE Intern. Semiconductor Laser Conf., Davos, Sept. 1990, pp. 44–45.
[10] D.Z. Garbuzov, N.Y. Antonishkis, A.D. Bondarev, S.N. Zhigulin, A.V. Kochergin, N.I. Katsavets and E.U. Rafailov, IEEE J. Quantum Electron. QE-27 (1991) 1531.
[11] Z.L. Liau, S.C. Palmateer, S.H. Groves, J.N. Walpole and L.J. Missaggia, Appl. Phys. Letters 60 (1992) 6.
[12] J.M. Kuo, Y.K. Chen, M.C. Wu and M.A. Chin, Appl. Phys. Letters 59 (1991) 2783.
[13] W.T. Tsang, Chemical beam epitaxy, in: VLSI Electronics Microstructure Science, Vol. 21, Ed. N.G. Einspruch (Academic Press, New York, 1989) ch. 6, pp. 255–357.
[14] W.T. Tsang, J. Crystal Growth 111 (1991) 529.
[15] J.C. Garcia, P. Maurel, P. Bove and J.P. Hirtz, J. Appl. Phys. 69 (1991) 3297.
[16] H.K. Choi and C.A. Wang, Appl. Phys. Letters 57 (1990) 321.
[17] N. Chand, E.E. Becker, J.P. van der Ziel, S.N.G. Chu and N.K. Dutta, Appl. Phys. Letters 58 (1990) 1704.
[18] R.L. Williams, M. Dion, F. Chatenoud and K. Dzurko, Appl. Phys. Letters 58 (1991) 1816.